



Microbial influence in Spanish bentonite slurry microcosms: Unveiling a-year long geochemical evolution and early-stage copper corrosion related to nuclear waste repositories[☆]

Marcos F. Martinez-Moreno^{a, *}, Cristina Povedano-Priego^a, Mar Morales-Hidalgo^a, Adam D. Mumford^b, Elisabet Aranda^c, Ramiro Vilchez-Vargas^d, Fadwa Jroundi^a, Jesus J. Ojeda^b, Mohamed L. Merroun^a

^a Faculty of Sciences, Department of Microbiology, University of Granada, Granada, Spain

^b Department of Chemical Engineering, Faculty of Science and Engineering, Swansea University, Swansea, United Kingdom

^c Institute of Water Research, Department of Microbiology, University of Granada, Granada, Spain

^d Medical Department II, University Hospital, Ludwig-Maximilians-Universität, Munich, Germany

ARTICLE INFO

Keywords:

DGR
Spanish bentonite
Microbial diversity
Electron donors/acceptor
Copper corrosion

ABSTRACT

The deep geological repository (DGR) concept consists of storing radioactive waste in metal canisters, surrounded by compacted bentonite, and placed deeply into a geological formation. Here, bentonite slurry microcosms with copper canisters, inoculated with bacterial consortium and amended with acetate, lactate and sulfate were set up to investigate their geochemical evolution over a year under anoxic conditions. The impact of microbial communities on the corrosion of the copper canisters in an early-stage (45 days) was also assessed. The amended bacterial consortium and electron donors/acceptor accelerated the microbial activity, while the heat-shocked process had a retarding effect. The microbial communities partially oxidize lactate to acetate, which is subsequently consumed when the lactate is depleted. Early-stage microbial communities showed that the bacterial consortium reduced microbial diversity with *Pseudomonas* and *Stenotrophomonas* dominating the community. However, sulfate-reducing bacteria such as *Desulfocurvibacter*, *Anaerosolibacter*, and *Desulfosporosinus* were enriched coupling oxidation of lactate/acetate with reduction of sulfates. The generated biogenic sulfides, which could mediate the conversion of copper oxides (possibly formed by trapped oxygen molecules on the bentonite or driven by the reduction of H₂O) to copper sulfide (Cu₂S), were identified by X-ray photoelectron spectroscopy (XPS). Overall, these findings shed light on the ideal geochemical conditions that would affect the stability of DGR barriers, emphasizing the impact of the SRB on the corrosion of the metal canisters, the gas generation, and the interaction with components of the bentonite.

1. Introduction

The global challenge of managing high-level radioactive waste (HLW) has led to the consideration of the Deep Geological Repository (DGR) as the internationally accepted option for this purpose (WNA, World Nuclear Association, 2021). The main objective is to preserve the long-term integrity and the safety performance of these repositories for periods spanning from several hundreds to millions of years, ensuring that no residual radioactive materials reach the surrounding environment (Batandjieva et al., 2009). The multi-barrier design of DGR consists

of a buffering and sealing bentonite-based material surrounding the waste-containing metal canisters that will be placed several hundred meters underground in a stable geological formation to ensure safety until the radiotoxicity diminishes to levels similar to natural ones (Ojovan and Steinmetz, 2022). The nature of the barriers depends on the particular strategy adopted by each country. Copper-coating metal canisters have been proposed, or already implemented, by countries such as Canada, Korea, Sweden, and Finland (Hall et al., 2021). In addition, compacted bentonite clay was selected as the most appropriate buffer and sealing material. This clay provides mechanical support for

[☆] This paper has been recommended for acceptance by Hocheol Song.

* Corresponding author.

E-mail address: mmartinezm@ugr.es (M.F. Martinez-Moreno).

<https://doi.org/10.1016/j.envpol.2024.124491>

Received 15 April 2024; Received in revised form 19 June 2024; Accepted 1 July 2024

Available online 2 July 2024

0269-7491/© 2024 The Authors. Published by Elsevier Ltd. This is an open access article under the CC BY license (<http://creativecommons.org/licenses/by/4.0/>).

canisters, prevents groundwater infiltration, retards radionuclides diffusion, and seals canisters in the event of rupture or cracks (García-Romero et al., 2019). In Spain, bentonite from Almeria (FEBEX) has been proposed as buffer material for Spanish DGR (Huertas et al., 2021; Villar et al., 2006).

Since bentonites are not sterile, understanding the structure and composition of the microbial community within this clay could provide insights into its potential impact on the long-term stability and safety of the DGR barriers (Meleshyn, 2014). Microorganisms may compromise the mineralogy and chemistry of the bentonite buffer and the integrity of the metal canisters due to microbially influenced corrosion (MIC) via biofilm formation or corrosive metabolite production (Ruiz-Fresneda et al., 2023). Moreover, microbial metabolism may contribute to the production of hydrogen, methane, and carbon dioxide, affecting the gas phase that would increase the pressure within the DGR (Guo & Fall 2021; Bagnoud et al., 2016).

Once the DGR is sealed, the gradual depletion of oxygen will occur due to factors such as microbial activity and metal canister corrosion, leading to the establishment of an anoxic environment (Payer et al., 2019; Keech et al., 2014). In this context, certain anaerobic bacteria such as sulfate-reducing bacteria (SRB) and iron-reducing bacteria (IRB) could remain metabolically active. These bacteria may have adverse consequences, including the promotion of MIC, the reduction of Fe(III) to Fe(II) in smectite (the major mineral in bentonites), and the reduction of sulfate to sulfide (a key agent in copper corrosion) (Pentráková et al., 2013; Liu et al., 2012; Shelobolina et al., 2003). Sulfide production, attributed to SRB activity, is more likely to occur further away from the canisters under conditions that favor SRB growth, such as lower temperatures and higher water activity (Bengtsson and Pedersen, 2017). This biogenic sulfide could diffuse through the biologically inactive section of the sealing materials and influence the nature and rate of canister-surface corrosion.

Although the bentonite will be in the form of compacted blocks within the DGR, which is expected to suppress microbial activity, it is necessary to consider all possible scenarios. Therefore, to understand the impact of the microbial activity, including the indigenous microorganisms, on Spanish bentonite over the short term, optimal conditions for microbial growth, representing a worst-case scenario for a DGR, were simulated. In this study, bentonite slurry anaerobic microcosms were amended with acetate, lactate, and sulfate (electron donors and acceptor, respectively) to stimulate microbial activity. Hence, this study aims to comprehensively examine the impact of microorganisms on the geochemical evolution of complex bentonite slurry systems for one year of anoxic incubation. Additionally, the microbial communities and their influence on copper corrosion in an early state (45 days) of incubation within the microcosms were investigated.

Our results emphasize the role of the microorganisms present in the bentonite, which could provide optimal growth conditions in the event of an influx of nutrients due to the filtration of water in the bentonite.

2. Materials and methods

2.1. Bentonite sampling

The bentonite was aseptically collected from El Cortijo de Archidona site in Almeria (Spain) in February 2020 (maximum depth: ~ 80 cm). Subsequently, the bentonite was aseptically disaggregated, dried and ground to achieve a uniform powder following the procedure by Martínez-Moreno et al. (2023). The chemical composition of the initial bentonite is specified in the Supplementary Table S1.

2.2. Microcosms assembly and sampling

Procedures related to copper material and mini-canister (Cu-mCan) assembly, elaboration of the different solutions, and BPAS consortium information and culture conditions are detailed in Supplementary

Material.

Microcosms were set up following the procedure described by Povedano-Priego et al. (2023) with some modifications. Fifty g of ground bentonite was added to 250 mL borosilicate glass bottles previously autoclaved. Solutions of acetate, lactate and sulfate (section 1.1 of Supplementary Material) were supplemented in the electron donors/acceptor-containing (eD) microcosms with a final concentration of 30 mM, 10 mM, and 20 mM, respectively. Additionally, the bacterial consortium-containing (BC) bottles were spiked with a BPAS consortium (section 1.2 of Supplementary Material) with an initial OD₆₀₀ of 0.4 for each bacterial strain (*Bacillus* sp. BII-C3, *Pseudomonas putida*, *Amycolatopsis ruanii*, and *Stenotrophomonas bentonitica*). The final volume of the microcosms was calculated considering the solutions added and then were filled up to 230 mL with the equilibrium water (EW) (section 1.1 of Supplementary Material). Finally, for corrosion studies, three sterilized high-purity oxygen-free Cu-mCan (section 1.3 of Supplementary Material) were deposited into each microcosm.

Different treatments were considered to study the impact of three parameters (sample code between brackets): i) bentonite and heat-shocked bentonite (B and StB), ii) acetate:lactate:sulfate addition (eD), and iii) the inoculation of the BPAS bacterial consortium (BC). Although tyndallization (heat-shock) is not the optimal method for sterilizing bentonite (Martínez-Moreno et al., 2024)), StB bentonites were tyndallized (110 °C for 45 min, 3 consecutive days) to reduce the presence and activity of autochthonous bacteria. A total of 24 microcosms were elaborated (8 treatments in triplicate). The sample ID and characteristic of the treatments are summarized in Table 1.

Once the microcosms were completed, the borosilicate bottles were sealed with butyl-rubber stoppers and degassed with N₂ to create anoxic conditions. Subsequently, the microcosms were incubated at 28 °C for one year. The workflow of the microcosms set-up is shown in Fig. 1. Samples from the different components (supernatant, bentonite slurry, and Cu-mCan) were recovered aseptically within an anaerobic chamber for the different analyses.

2.3. Geochemical analyses of the microcosm supernatants

For the evolution of geochemical analysis, supernatant (liquid phase) aliquots from each microcosm were collected at 45, 90, 135, and 365 days of incubation under anoxic conditions, and filtered with 0.22 µm cellulose-acetate filter. The pH was measured by Advanced Digital Handheld Portable Meter HQ40D (Hach) previously calibrated with commercial reference solutions (4.00 and 7.00).

Acetate, lactate, and sulfate concentrations in the supernatants from the amended samples (eD) were quantified by High Pressure Ion Chromatography (HPIC) to understand the chemical evolution of these added compounds. The analysis was performed in a 925 Eco ICE, Methrom Hispania (Herisau, Switzerland) coupled with an IC conductivity detector, a Metrohm Suppressor Module (MSM), 250 µL injection loop with

Table 1

Experimental conditions and sample ID of the different treatments. All free-oxygen microcosms incorporated three Cu mini-canisters (Cu-mCan) and were elaborated in triplicate. A:L:S: acetate, lactate, and sulfate concentrations; BPAS: bacterial consortium; +: presence; -: absence.

Sample ID	Bentonite	A:L:S (mM)	BPAS
B.eD.BC	Non-heat-shocked	30:10:20	+
B.BC		–	+
B.eD		30:10:20	–
B		–	–
StB.eD.BC	Heat-shocked	30:10:20	+
StB.BC		–	+
StB.eD		30:10:20	–
StB		–	–

Glossary: B: bentonite, StB: heat-shocked bentonite, eD: addition of electron donors and sulfate, BC: spiked with bacterial consortium.

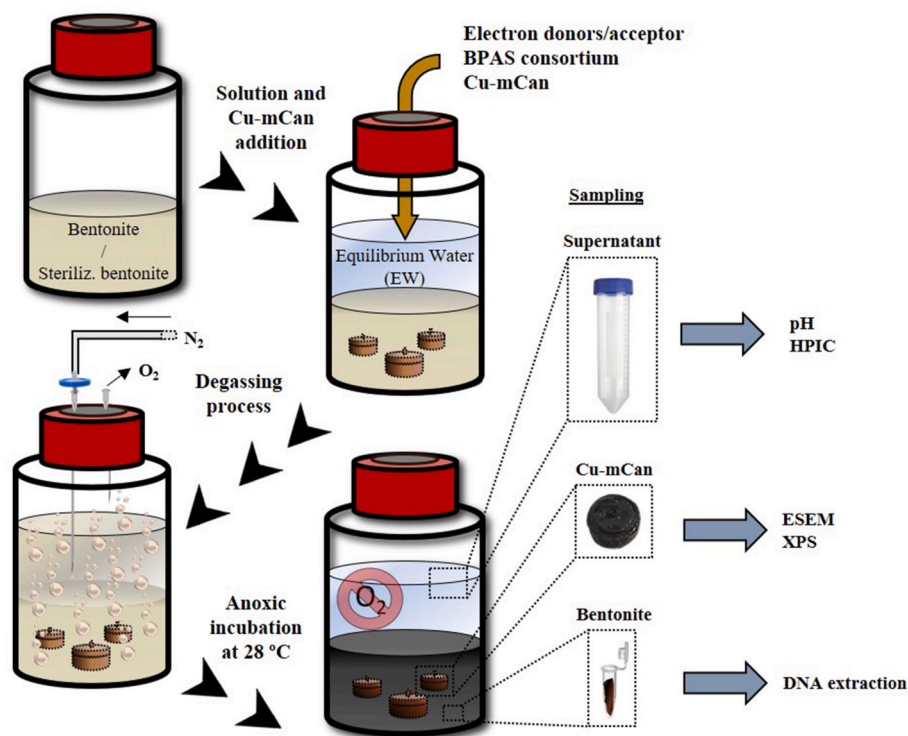


Fig. 1. Microcosms workflow, N₂ degassing process (anoxic conditions), and sampling for the different analyses.

peristaltic pump, Metrohm high pressure pump with purge valve and 919 UF autosampler. Before injection, samples were 0.22 μm filter-sterilized and diluted in ultrapure water. Measurement specifications are detailed in section 1.4 of the Supplementary Material.

2.4. DNA extraction, sequencing, and computational procedure

DNA extraction was performed for each microcosm at 45 days incubation following the procedure detailed in Povedano-Priego et al. (2021) in order to characterize the microbial community within the microcosms in an early-stage incubation and their implication on the alteration of the Cu-mCans. Subsequently, the extracted DNA concentration was determined using Qubit 3.0 Fluorometer (Life Technology, Invitrogen™).

For the library preparation, two consecutive PCR reactions were carried out for each sample using a combination of regular and barcoded fusion primers to amplify the V5 – V6 variable regions of the 16S rRNA gene (see details in section 1.5 of Supplementary Material). Libraries were sequenced using the MiSeq Illumina platform (2 × 250 bp, Hayward, California, USA).

FastaQ files were processed and normalized using “dada2” and “phyloseq” packages, respectively, in R 4.2.1 software (R Core Team, 2022). Bayesian classification was employed to assign a taxonomic affiliation to the phylotypes (80% pseudo-bootstrap threshold). The relative abundances and alpha diversity indices were conducted using Explicit 2.10.5 (Robertson et al., 2013). To assess the similarity between samples at genus level, a matrix based on the Bray-Curtis algorithm was used, and subsequent similarity between samples was performed through principal coordinate analysis (PCoA) using Past 4 software (Hammer, 2001). Furthermore, a heatmap was performed to visualize taxa with more than 0.50% relative abundance. For this purpose, the ‘heatmap.2’ function was employed in R software.

2.5. Surface characterization of the copper mini canisters (Cu-mCan)

After 45 days of anoxic incubation, the Cu-mCan were collected from

the microcosms, unscrewed, and dried under anoxic atmosphere. To visualize corrosion compounds on the surface, the base of the Cu-mCan was metallized with a carbon coating through evaporation by an EMI-TECH K975× Carbon Evaporator for analysis by High Resolution Scanning Electron Microscopy (HRSEM) with an AURIGA Carl Zeiss SMT microscope associated with a qualitative and quantitative energy dispersive X-ray (EDX) microanalysis.

Moreover, no previous preparation was applied to the lids of the Cu-mCan for spectroscopic analysis. The chemical analysis by X-ray photoelectron spectroscopy (XPS) of the lids’ surfaces was conducted on a Kratos AXIS Supra Photoelectron Spectrometer. Spectra acquisition and detailed information are shown in section 1.6 of the Supplementary Material. Finally, CasaXPS 2.3.22 software (Fairley, 2019) was used to fit the peaks of the XPS spectra. All binding energies were offset by referencing the adventitious carbon C1s peak (285 eV).

3. Results and discussion

3.1. Water chemistry evolution

Untreated bentonite is expected to have an initial alkaline pH around 9.00 due to its innate buffering capacity (Povedano-Priego et al., 2019; Rozalén et al., 2009). After one-year incubation, pH values tended to stabilize between 7.51 and 8.37 in all treatments, in contrast to the initial values (Supplementary Fig. S2). The observed pH decrease could be due to leaching of the bentonite or microbial activity through the generation of gases such as hydrogen (H₂), methane (CH₄), and carbon dioxide (CO₂) (Fernández-Díaz 2004; Povedano-Priego et al., 2019; Bagnoud et al., 2016).

Lactate was the first electron donor to be consumed (Fig. 2A). Complete depletion was achieved at 45 days in the microcosms spiked with the bacterial consortium (B.eD.BC) in contrast to its heat-shocked counterpart StB.eD.BC, where lactate was consumed after 45 days. In the microcosms without the bacterial consortium, lactate was slowly consumed reaching complete depletion at 135 days (B.eD) and 365 days (StB.eD). Regarding acetate evolution (Fig. 2B), in the sample B.eD.BC

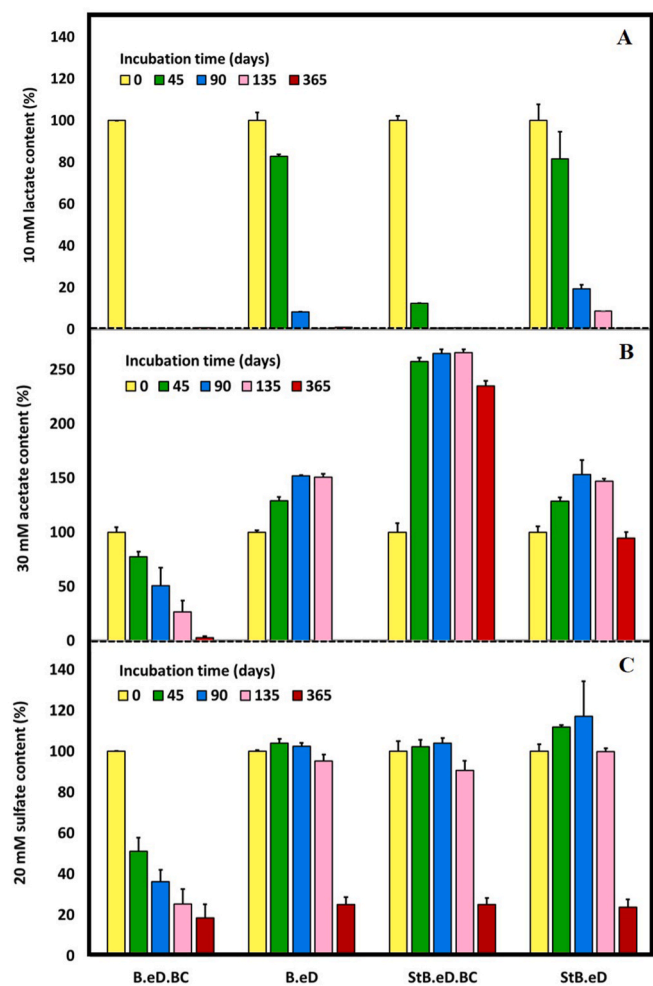


Fig. 2. Evolution of the initial concentration of 10 mM lactate (A), 30 mM acetate (B), and 20 mM sulfate (C) content recorded in Spanish bentonite microcosms incubated anaerobically at 28 °C for 1 year. Data showed the mean values with standard derivations measured from three independent replicates. Glossary: B: bentonite, StB: heat-shocked bentonite, eD: addition of electron donors and sulfate, BC: spiked with bacterial consortium.

acetate was gradually depleted following the consumption of lactate being nearly exhausted after one year-incubation. In the other treatments, acetate initially increased before being consumed, with complete depletion occurring around one year-incubation in B.eD. This could suggest that acetate is produced from lactate consumption and subsequently used as an electron donor. Sulfate consumption (Fig. 2C) was highest in the non-heat-shocked samples containing the bacterial consortium (~50% in B.eD.BC). In the samples B.eD, StB.eD.BC, and StB.eD, sulfate levels remained relatively stable for most of the incubation period, only decreasing to about 20–30% after one year.

In general terms, the tyndallization of the bentonite (heat-shocked samples) seems to slow down the dynamics of lactate and acetate, and sulfate reduction when compared with the non-heat-shocked samples. This indicated that tyndallization adversely affects microbial activity. Moreover, the bacterial consortium seemed to enhance lactate consumption and acetate production/consumption.

The conversion of lactate to acetate, in the absence of sulfate reduction, could occur via lactate fermentation to acetate and propionate, or its incomplete oxidation to acetate coupled with iron reduction (Park et al., 2024). The consumption of sulfate in the sample B.eD.BC is supported by the work of Matschiavelli et al. (2019). They observed a decrease in lactate and sulfate concentrations concomitant with acetate formation in B25 Bavarian bentonite microcosms. Their study deduced

that through the reductive pathway of acetyl-CoA, lactate is incompletely oxidized to acetate with the concurrent reduction of sulfate to hydrogen sulfide. The presence of fissures in the bentonite (white arrows in Fig. 3) and the formation of small bubbles in the microcosms could be related to gas generated by microbial activity. The rotten egg odor after sampling could also support the hydrogen sulfide (H₂S) formation (He et al., 2011). The visual color changes observed in the bentonite microcosms during the incubation are also presented in Fig. 3. A shift towards black hues was evidenced in the treatment containing the bacterial consortium (B.eD.BC), with this transformation occurring at a slower rate when the bentonite was heat-shocked (StB.eD.BC). Subsequently, the treatments lacking the bacterial consortium (B.eD, and StB.eD) exhibited similar color changes, although with lower progression. The alteration in the color of the bentonite may be linked to the generation of H₂S, a byproduct of bacterial activity, which can react with iron and lead to the formation of black precipitates of reduced iron species (Miettinen et al., 2022; Matschiavelli et al., 2019).

3.2. Characterization of microbial communities in an early incubation stage

The microbial communities of the bentonite microcosms were characterized to get a thorough comprehension of early-stage geochemical changes and their influence on copper corrosion. Thus, the total DNA from the different bentonite microcosms after 45 days of anoxic incubation was extracted and sequenced in triplicate (duplicate in sample StB.eD). The structure and composition of bacterial communities in the different treatments was characterized: tyndallized (StB), presence of electron donors/acceptor (eD), and addition of the bacterial consortium (BC) in the early-stage of incubation (45 days) in order to study their influence in the corrosion of copper material.

For these samples, enough sequencing depth was achieved as shown by the rarefaction curves (Supplementary Fig. S3). A total of 412 phylotypes were detected and annotated in 13 phyla (98.06%) being Pseudomonadota (74.63%), Bacillota (19.74%), and Actinomycetota (2.67%) the most abundant phyla (Supplementary Table S4). At genus level, the phylotypes were annotated in 110 OTUs (Supplementary Table S5) with *Pseudomonas* (43.35%), *Stenotrophomonas* (13.41%), unclassified Clostridiales (4.75%), *Pseudoalteromonas* (4.64%), *Symbiobacterium* (4.24%), *Desulfocurvibacter* (3.08%), unclassified Bacillota (2.98%), and *Desulfuromonas* (2.89%) presenting the higher relative abundance in the pool of the samples.

Richness (Sobs), diversity (ShannonH and SimpsonD), and evenness (ShannonE) indices at the genus level of the samples are presented in Supplementary Table S3. The richness indices of non-heat-shocked treatments reveal higher values in samples lacking bacterial consortium, and these values are greater in the absence of electron donors and sulfate (richness values B > B.eD > B.eD.BC > B.BC). In contrast, the dynamics in the heat-shocked treatments (StB) seemed to be slightly different, with higher richness values in the samples amended with electron donors and sulfate, while the presence of the consortium seemed to affect the richness indices diminishing the effect of electron donors (richness values StB.eD > StB.eD.BC > StB > StB.BC). These results were supported by the diversity indices (ShannonH and SimpsonD) showing the same trends in the samples (Supplementary Table S3). The microcosms without bacterial consortium showed greater diversity values (ShannonH >3, and SimpsonD close to 1) than those spiked with the bacterial consortium (BC), indicating that the addition of this consortium resulted in a displacement of the indigenous bentonite microbial community and the dominance of specific taxa within the samples (ShannonH <3, and SimpsonD further from 1).

In order to analyze the dissimilarity and diversity distribution along the different microcosms considering the relative abundance at genus level, samples were grouped by a principal coordinate analysis (PCoA) based on Bray-Curtis distance (Fig. 4A). The dissimilarity between samples containing the bacterial consortium and those lacking it was

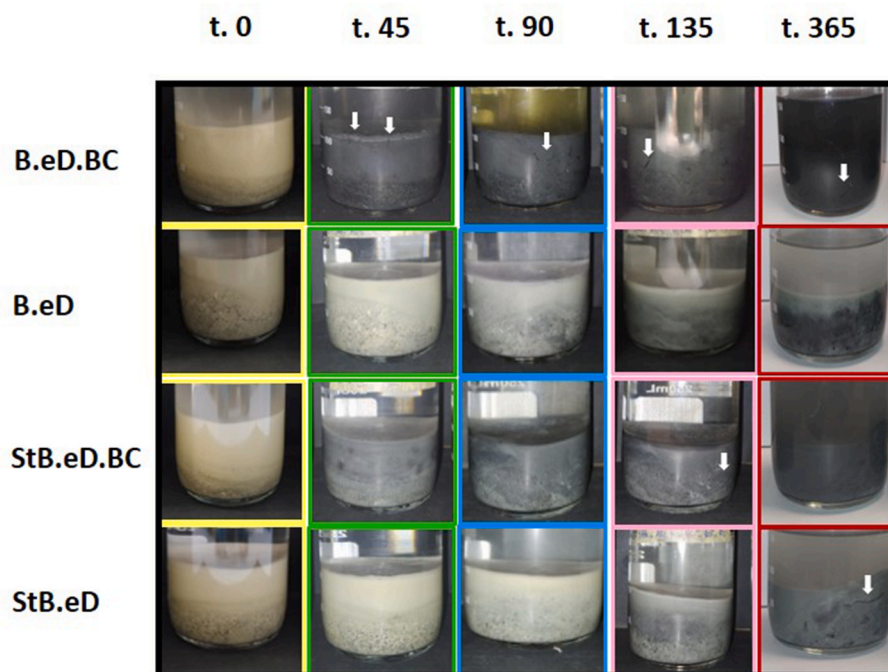


Fig. 3. Evolution of hyper-saturated Spanish bentonite microcosms before (yellow) and after 45 (green), 90 (blue), 135 (pink) and 365 (red) days of anaerobic incubation at 28 °C. White arrows indicate the development of fissures and cavities attributed to gas formation. Glossary: B: bentonite, StB: heat-shocked bentonite, eD: addition of electron donors and sulfate, BC: spiked with bacterial consortium. (For interpretation of the references to color in this figure legend, the reader is referred to the Web version of this article).

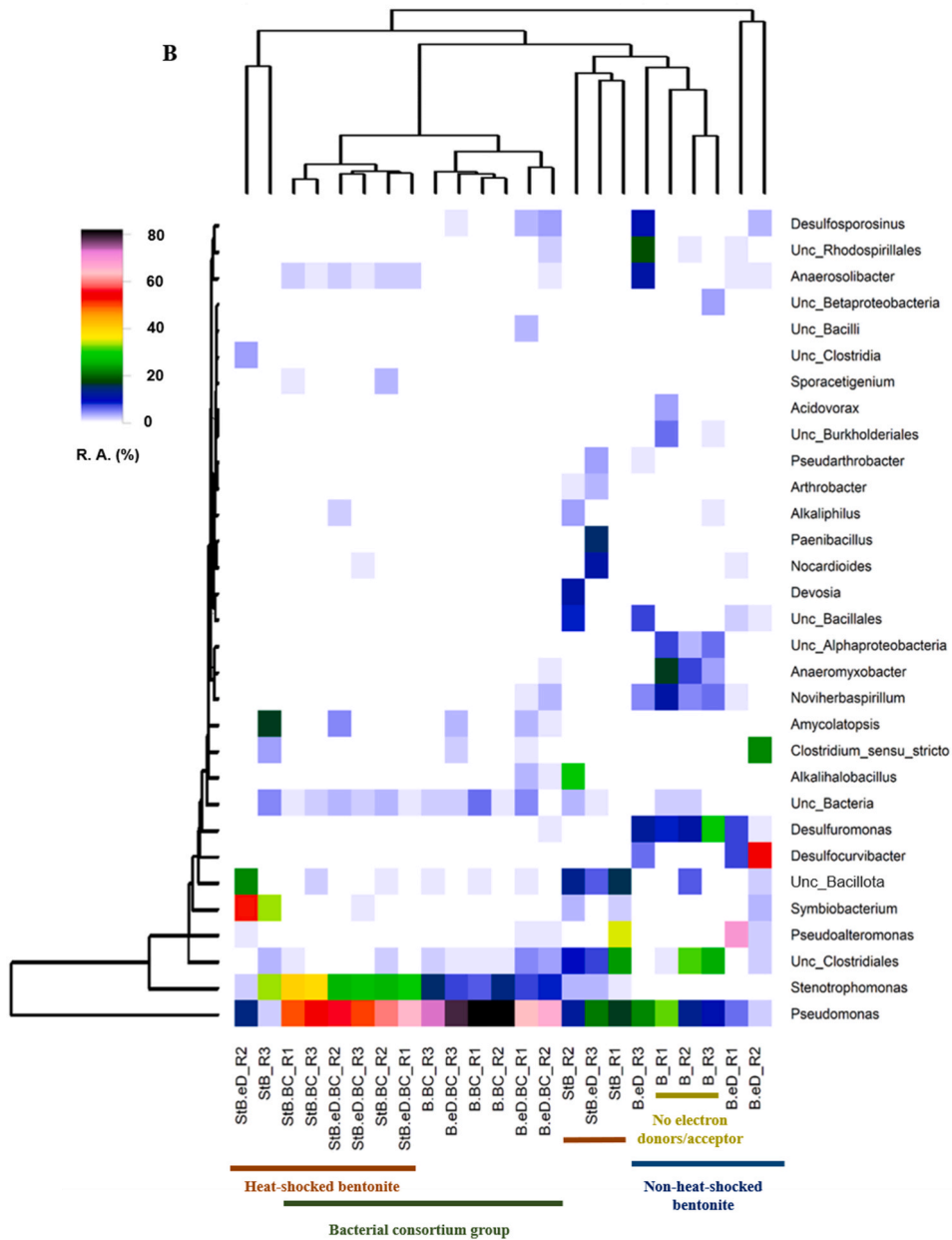
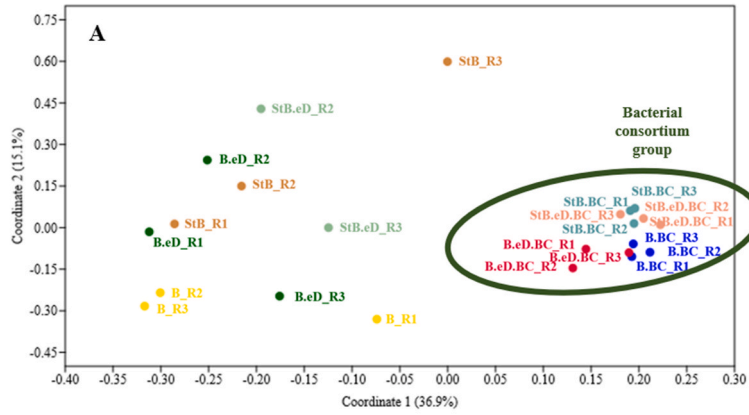
evidenced. The treatments containing bacterial consortium (BC samples) were grouped separately from the others, indicating that those lacking bacterial consortium showed a more heterogeneous distribution.

Moreover, a heatmap was constructed to confirm the similarity between samples (Fig. 4B). As observed, the clustering of BC samples was primarily attributed to the prevalence of bacterial genera from the BPAS consortium, notably *Pseudomonas* and *Stenotrophomonas*, which dominate the microbial communities of these microcosms. In contrast, for samples lacking a bacterial consortium, a slight differentiation was observed between samples with heat-shocked bentonite (StB) and those with non-heat-shocked bentonite (B), possibly due to the negative effect of the tyndallization process on the microbial diversity of the bentonite (Martínez-Moreno et al., 2023; Povedano-Priego et al., 2023). However, such differentiation was not observed when considering the absence or the presence (eD) of electron donors and sulfate. The main difference between microcosms unamended (B) and amended with electron donors and sulfate (B.eD) resided in the presence of bacterial genera such as *Pseudoalteromonas* (24.17%), *Desulfocurvibacter* (22.72%), *Anaerosolibacter* (4.54%), *Desulfosporosinus* (4.54%), and unclassified bacteria belonging to the highly diverse order of Bacillales (3.70%) in sample B.eD. Some strains of *Pseudoalteromonas* have adaptive mechanisms to tolerate low oxygen concentrations (Qin et al., 2011) or the ability to use acetate as a carbon source (Oh et al., 2011) which support the distribution of *Pseudoalteromonas* in this treatment. Moreover, the strictly anaerobes *Desulfocurvibacter*, *Anaerosolibacter* and *Desulfosporosinus* can use sulfate and/or iron as electron acceptor to grow in the presence of organic substrates (e.g., lactate) (Spring et al., 2019; Hong et al., 2015; Hippe and Stackebrandt, 2015).

As shown in the heatmap (Fig. 4B), the dominant genera in the consortium-spiked treatments (BC) were those of the consortium, *Pseudomonas* (54.59% – 78.88%) and *Stenotrophomonas* (34.96% – 8.10%) (Supplementary Table S5 and Fig. 5). *Amycolatopsis*, was detected in lower relative abundance in the BC microcosms exhibiting higher abundance in B.eD.BC and StB.eD.BC samples (2.31% and 2.05%, respectively). In contrast, the presence of *Amycolatopsis* was lower or

undetectable in the samples without electron donors and sulfate: 0.12% and 0% (B.BC and StB.BC, respectively). Regarding *Bacillus* genus, it was outside the detection range in the samples. *Pseudomonas putida* and *Stenotrophomonas bentonitica* are bacterial strains capable of growing or maintaining their activity under anaerobic conditions, while also exhibiting the ability to use acetate and/or lactate as a carbon source (Freikowski et al., 2010; Sanchez-Castro et al., 2017). *Pseudomonas* was also detected in the microcosms without bacterial consortium with a remarkable relative abundance of 9.80% (B.eD), 19.11% (B), 16.48% (StB.eD), and 9.91% (StB). On the other hand, *Stenotrophomonas* was only detected in the heat-shocked treatments (StB.eD and StB) with a 2.66% and 13.98% of relative abundance, respectively.

As observed in the chemical evolution data (Fig. 2), the samples spiked with the bacterial consortium (BC) showed the highest rate of lactate consumption after 45 days of incubation, and the highest consumption (B.eD.BC) or production (StB.eD.BC) of acetate. *Pseudomonas* and *Stenotrophomonas* could be key contributors to the observed trend of lactate consumption and acetate production/consumption in the samples amended with electron donors/acceptor (eD) (Essén et al., 2007; Eschbach et al., 2004; Ruiz-Fresneda et al., 2019; Sanchez-Castro et al., 2017). Moreover, in sample B.eD.BC, the presence of the sulfate-reducing bacterium *Desulfosporosinus* (Supplementary Table S5 and Fig. 5) was evidenced (2.62%). This bacterium is involved in the incomplete oxidation of substrates, such as lactate to acetate, and in the use of sulfate as a terminal electron acceptor (Spring and Rosenzweig, 2006). This fact could be linked to the sulfate consumption (~ 50%) within this sample at the 45-day mark (Fig. 2C). In contrast, sample StB.eD.BC did not show sulfate reduction (Fig. 2C). This could be attributed to the absence of *Desulfosporosinus* in this treatment and the presence of the IRB and SRB *Anaerosolibacter* (1.83%; Supplementary Table S4 and Fig. 4). The dominance between sulfate reduction and iron reduction depends on pH, iron crystallinity, and their concentrations. In this experiment, with a neutral pH and a high sulfate concentration, sulfate reduction is likely more favorable. Therefore, the presence of this bacterial genus may indicate that the redox conditions are not yet optimal



(caption on next page)

Fig. 4. A: principal coordinate analysis (PCoA) plot showing the dissimilarity of bacterial communities at genus level from bentonite-slurry microcosms after 45 days of anoxic incubation. **B:** Heatmap representing genus-level relative abundance and clustering based on Manhattan distance of the slurry-bentonite microcosms after 45 days of incubation. The 3.3% cut off based on the maximums represents the 31 most abundant genera. The relative abundance of each genus is shown with different colors (the warmer the color, the greater relative abundance). Glossary: B: bentonite, StB: heat-shocked bentonite, eD: addition of electron donors and sulfate, BC: spiked with bacterial consortium. (For interpretation of the references to color in this figure legend, the reader is referred to the Web version of this article.)

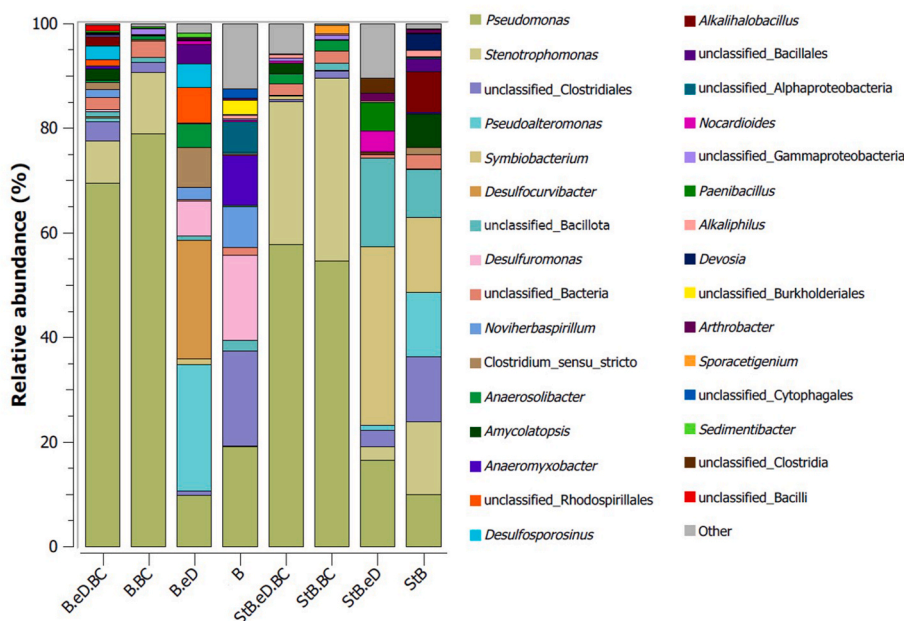


Fig. 5. OUT relative abundance of bacterial communities from the bentonite slurry microcosms. Cut off: 0.20% of relative abundance. Stacked bars show averages of biological replicates. Glossary: B: bentonite, StB: heat-shocked bentonite, eD: addition of electron donors and sulfate, BC: spiked with bacterial consortium.

for sulfate reduction to occur.

The addition of electron donors and sulfate in samples not spiked with bacterial consortium appears to enhance the prevalence of bacterial genera such as *Desulfocurvibacter* (obligate anaerobic SRB that incompletely oxidize organic substrates to acetate), *Pseudoalteromonas* (IRB under low content of oxygen), *Anaerosolibacter* (IRB and SRB), and *Desulfosporosinus* (anaerobic bacteria that reduce sulfate through the incomplete oxidation of lactate to acetate) (Spring et al., 2019; Cheng et al., 2019; Stackebrandt et al., 1997). These genera exhibited high diversity in sample B.eD (22.72%, 24.17%, 4.54%, and 4.54%, respectively), whereas they were not detected, or detected in a very low abundance, in sample B (< 0.2%) (Supplementary Table S5 and Fig. 5). Despite the presence of SRB in the B.eD treatment, no observable sulfate consumption was detected (Fig. 2C). This lack of consumption could be attributed to the limited time available for this process (45 days), as IRB such as *Pseudomonas* (9.80%), *Anaerosolibacter* (4.54%), and *Pseudoalteromonas* (24.17%) might be actively engaged in the fermentation of lactate to acetate and propionate as suggested by Park et al. (2024). The resulting acetate could be then used to promote the reduction of Fe (III) to Fe(II). This reduction process may continue until the redox conditions within the microcosms become favorable for sulfate reduction. Moreover, the most abundant genera in sample B were *Pseudomonas* (19.11%), unclassified Clostridiales (18.25%), *Desulfuromonas* (16.37%), *Anaeromyxobacter* (9.57%), and *Noviherbaspirillum* (7.77%) being less abundant in the B.eD treatment (Supplementary Table S5 and Fig. 5). *Desulfuromonas* has the capacity to couple the oxidation of acetate and lactate with the reduction of sulfate (Liesack and Finster, 1994). The occurrence of *Pseudomonas*, *Anaeromyxobacter*, and *Noviherbaspirillum*, all facultative anaerobes, indicated their capability to use acetate and/or lactate as carbon sources (Shrestha et al., 2022; Sanford et al., 2002; Ishii et al., 2017). On the other hand, *Symbiobacterium* was the

most abundant genus within the heat-shocked samples without bacterial consortium (StB.eD: 34.11%, and StB: 14.39%). Bacterial species within this genus, including *S. turbinis* and *S. terracilitae*, are moderately anaerobic and thermophilic, with the characteristic of occasional endospore formation. Furthermore, these bacteria are capable of producing acetate as end product (Shiratori-Takano et al., 2014). The presence of this bacterial genus within the StB.eD.BC sample could suggest a contribution to the increase in acetate content observed in this treatment after 45 days of incubation (Fig. 2B). Moreover, in the heat-shocked sample without a bacterial consortium (StB), *Stenotrophomonas* (13.98%), unclassified Clostridiales (12.39%), *Pseudoalteromonas* (12.36%), *Pseudomonas* (9.91%), unclassified Bacillota (9.12%), the facultative anaerobic *Alkalihalobacillus* (7.81%), and *Amycolatopsis* (6.44%), were the most prevalent bacterial genera following *Symbiobacterium*.

In summary, the addition of the bacterial consortium had an impact on the shift of indigenous bentonite microbial community. However, it is noteworthy that only *Pseudomonas* and *Stenotrophomonas* managed to persist and prevail in the BC microcosms after 45 days of incubation, whereas *Amycolatopsis* and *Bacillus* exhibited lower abundances or fell below the detection threshold of the sequencing procedure. Furthermore, the presence of specific bacterial genera was intricately linked to the consumption of lactate, acetate and sulfate within the samples at 45 days of anoxic incubation. Given the complexity and heterogeneity of the bacterial diversity, it is plausible that each bacterium may exhibit a different metabolic profile. Thus, the total reaction computation observed in Fig. 2 does not align stoichiometrically with a simple system or an isolated bacterial strain study. Some bacteria (e.g., *Desulfosporosinus*) are able to partially oxidize lactate, associated with sulfate reduction, leading to the production of acetate. This acetate, in turn, could serve as a carbon source for other bacterial groups. Conversely,

the addition of electron donors and sulfate appears to stimulate the presence of IRB and SRB (e.g., *Desulfocurvibacter*, *Pseudoalteromonas*, *Anaerobolobacter*, and *Desulfosporosinus*). These groups of bacteria are involved in the corrosion of metal canisters within the DGR (Schutz et al., 2015; Bengtsson and Pedersen, 2017). However, the sulfate consumption was only detected at 45 days of incubation in the sample B.eD.BC (~ 50%). Hence, it is crucial to investigate the potential impact of these bacterial groups on the corrosion of copper material and characterize the resulting products.

3.3. Characterization of the Cu canister surface in an early-incubation stage

In order to assess the influence of the microbial communities on the corrosion of the copper surface after 45-day incubation, the Cu-mCan were recovered from the studied microcosms. The metal surfaces were analyzed by microscopic and spectroscopic techniques (HRSEM, EDX, and XPS). Specifically, the analysis focused on Cu-mCan from microcosms with non-heat-shocked bentonite.

The Cu-mCan images of samples before (t. 0) and after 45 days and their HRSEM micrographs are shown in Fig. 6. The bentonite adhered to the copper surface was not removed to avoid the consequent

displacement of copper alteration-related products. Visually, the samples exhibited a different coloration after the incubation comparing with the blank (t. 0). The sample B.eD.BC presented a marked color transformation, shifting to dark gray-black hues, as well as some zones on Cu-mCan B.BC (Fig. 6B,C). At microscopic level, the samples after the incubation exhibit a heterogenous topography (second column, Fig. 6). The sample t. 0 displayed a uniform topography, revealing only the presence of Cu and C (attributed to the metallization process during the sample preparation). Furthermore, elemental EDX map of iron (Fe), carbon (C), aluminum (Al), sulfur (S), silicon (Si), oxygen (O), and copper (Cu) distribution of the selected areas is shown (Fig. 6). The signal of Si (pink), Fe (yellow), and Al (cyan) were attributed to the presence of bentonite adhered on the Cu surface. The detection of O (red) was mainly associated with Si (Si_xO) linked to the presence of bentonite.

Moreover, O was detected, to a lesser extent, on the copper surface (Cu_xO). Sulfur precipitates were only detected in the sample B.eD.BC, which may be related to Cu_xS (copper corrosion compounds) (Fig. 6B) linking with the data of sulfate consumption (~ 50%, Fig. 2C). Diffuse and more dispersed S accumulates were also detected in sample B.BC (Fig. 6C). Furthermore, in sample B.eD, the presence of oxygen seemed to be closely related to irregularities on the copper surface probably

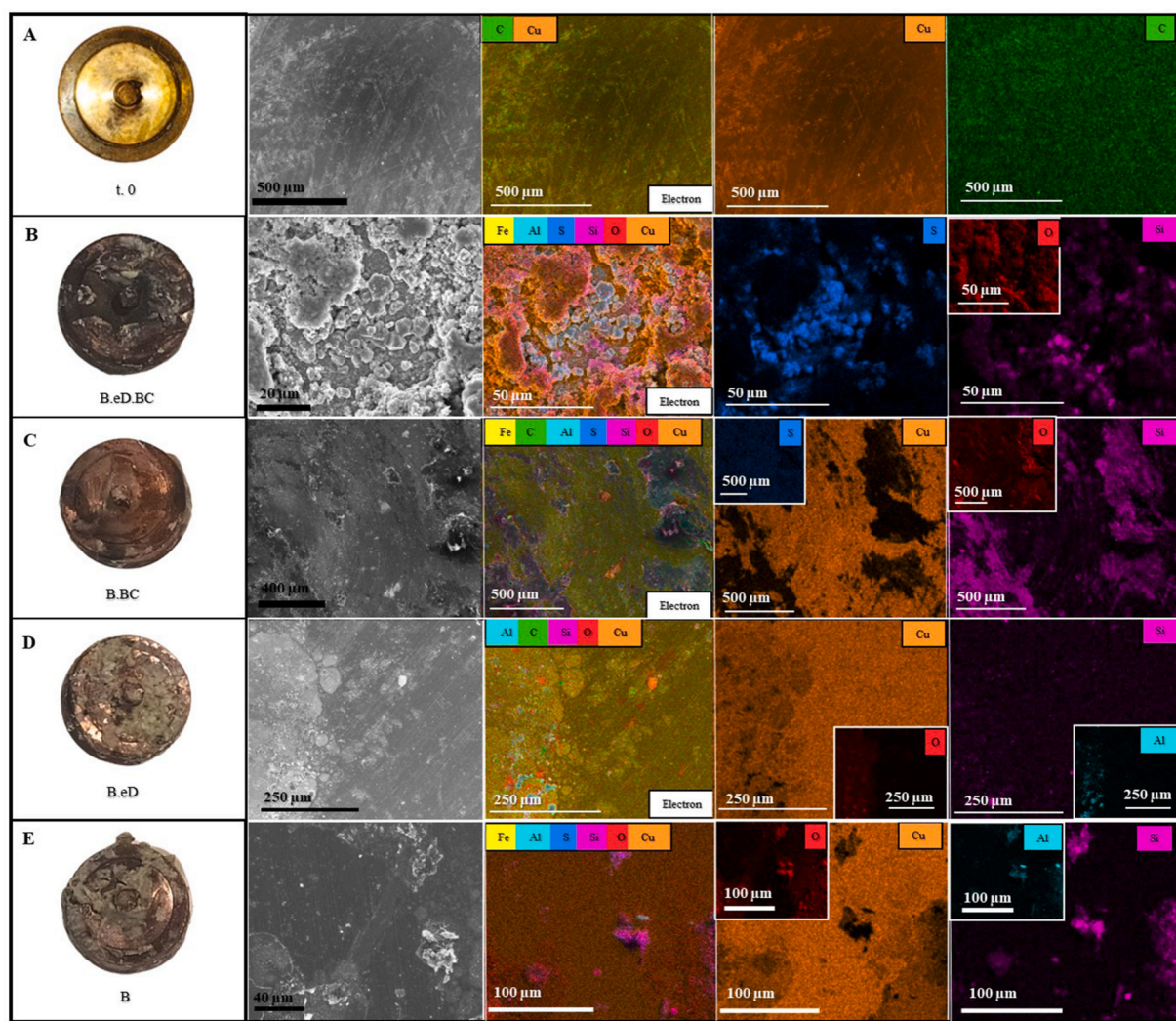


Fig. 6. Visual (first column), electron images (second column), and EDX maps of the Cu-mCan surface before experimental set-up (A) and after 45-days anoxic incubation from microcosms B.eD.BC (B), B.BC (C), B.eD (D), and B (E). EDX show the distribution of Cu (orange), Fe (yellow), S (dark blue), Si (pink), Al (cyan), O (red), and C (green) in the studied area. Glossary: B: bentonite, StB: heat-shocked bentonite, eD: addition of electron donors and sulfate, BC: spiked with bacterial consortium. (For interpretation of the references to color in this figure legend, the reader is referred to the Web version of this article.)

related to the presence of copper oxides (Cu_xO).

In order to identify the nature of the corrosion products, XPS analysis was undertaken in each Cu-mCan. Wide scans indicated the presence of Cu, C, O, Si, Na, Fe, Mg, and Al on all sample surfaces. Except for Cu,

these elements were attributed to bentonite adhered to the Cu-mCan's surfaces. High-resolution scans of the Cu 2p region exhibited elemental copper peaks (sharp peaks at approximately 933 eV and 953 eV, corresponding to $\text{Cu } 2p_{1/2}$ and $\text{Cu } 2p_{3/2}$, respectively), alongside the likely

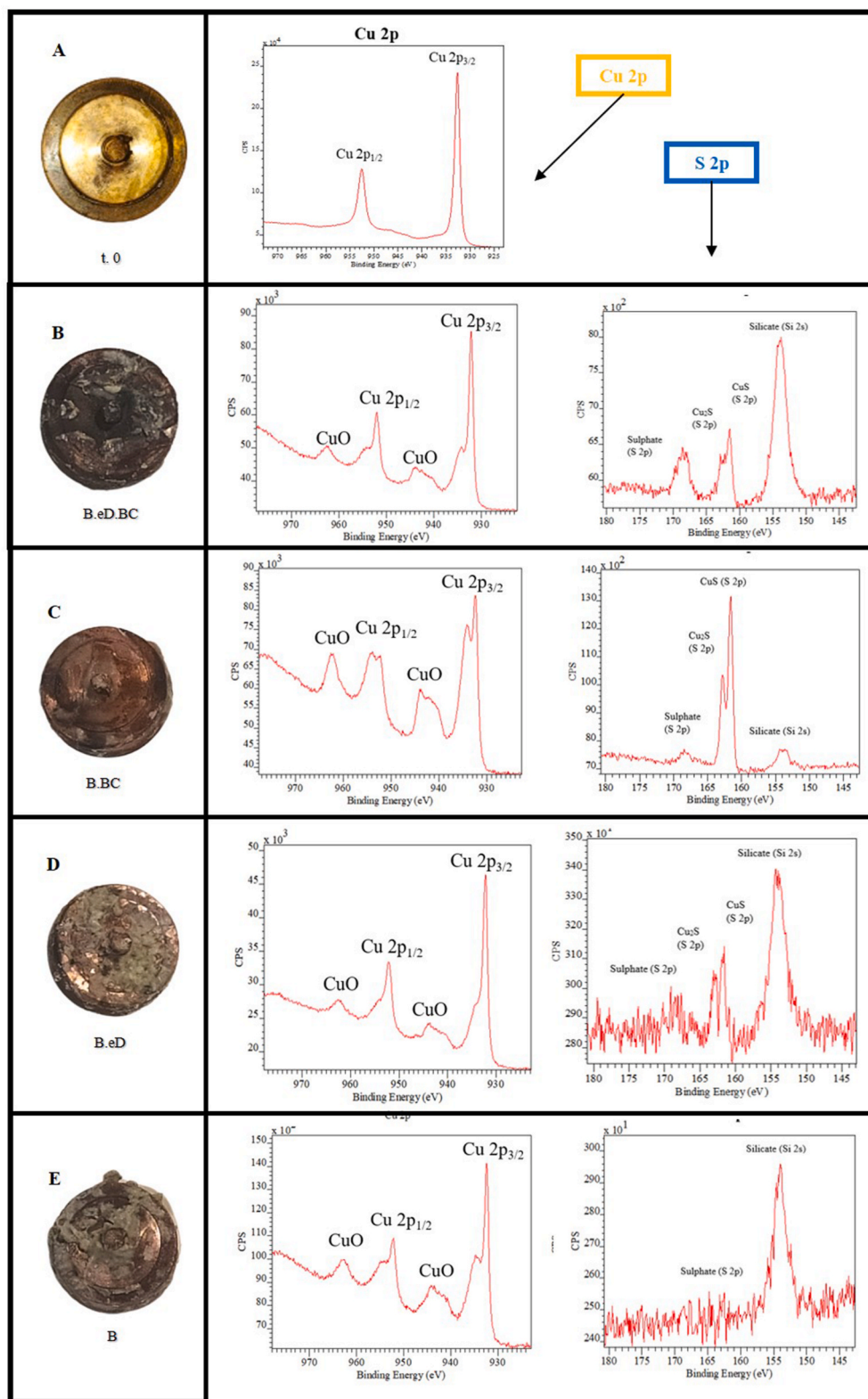


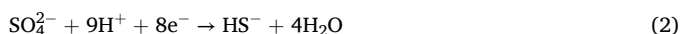
Fig. 7. High-resolution XPS spectra of the Cu 2p (977 eV–922 eV) and S 2p (180 eV–143 eV) regions of the Cu-mCan surface before experimental set-up (A) and after 45-days anoxic incubation from microcosms B.eD.BC (B), B.BC (C), B.eD (D), and B (E). Glossary: B: bentonite, StB: heat-shocked bentonite, eD: addition of electron donors and sulfate, BC: spiked with bacterial consortium.

presence of CuO (peaks around 943.49 eV and 962.89 eV) (Wagner et al., 1979), on all samples (Fig. 7). Further evidence for the existence of CuO included the separation of ~ 20 eV between Cu 2p_{1/2} and Cu 2p_{3/2} (Wagner et al., 1979). It should be noted that no CuO was detected on the surface of the Cu-mCan prior to microcosms set up (t. 0) as shown in the high-resolution spectra of the Cu 2p (Fig. 7).

The main signal of MIC under anoxic conditions on copper materials are Cu_xS mediated by the activity of SRB (Hall et al., 2021). Previous studies indicated that peaks for CuS were typically observed around 932.2 eV in high-resolution Cu 2p scans (Krylova & Andrulevičius, 2009). In order to delve deeper into the overshadow of this peak by the Cu 2p_{3/2} peak, high-resolution scans were conducted in the S 2p region, spanning from 143 eV to 180 eV. This revealed the presence of sulfur on samples B.BC, B.eD.BC, and B.eD (Fig. 7). In samples B.BC and B.eD.BC, peaks related to the presence of Cu₂S (around 163 eV) were seen. This is a known corrosion product produced as a result of HS⁻ excretion from SRB activity (Martinez-Moreno et al., 2023; Yu et al., 1990). Moreover, the peak at 161.4 eV was assigned to CuS (Kutty, 1991). The peak around 154 eV, presented in all the Cu-mCan after 45-days incubation, was attributed to Si 2s in the form of SiO₂ (silicate) belonging to the presence of the bentonite adhered on the copper surface (Clarke & Rizkalla, 1976).

Given that copper oxides (CuO) were identified on all Cu-mCan samples after 45 days of incubation, notably absent at t. 0, it can be inferred that the presence of oxygen, evidenced by CuO on the copper surface, occurred abiotically. The formation of the CuO species could be related to the oxygen molecules trapped in the bentonite, or driven by the reduction of H₂O from the EW (Burzan et al., 2022; Huttunen-Saarivirta et al., 2016). Conversely, the identification of Cu₂S in the samples resulted from microbial influence. This observation was particularly pronounced on the surface of Cu-mCan from the treatment with electron donors/acceptor and the bacterial consortium (B.eD.BC), followed by the treatment only spiked with the bacterial consortium (B.BC). Additionally, a lesser extent of Cu₂S detection was detected in the treatment supplemented only with electron donors/acceptor (B.eD). In contrast, Cu₂S was not detected in treatment B (untreated bentonite) (Figs. 6 and 7). Moreover, microscopic examination revealed the presence of precipitates of Cu₂S compounds exclusively in Cu-mCan from the treatment B.eD.BC (Fig. 6), aligning with the heightened presence of SRB within this treatment (Fig. 5 and Supplementary Table S5).

The production of sulfide through the reduction of sulfate is kinetically hindered under standard abiotic conditions of temperature and pressure (Cross et al., 2004). Thus, the presence of sulfide is likely to be attributed to the activity of SRB (Bengtsson and Pedersen, 2017). Under anoxic conditions SRB can oxidize lactate as electron donor (Eq. (1)) coupled to sulfate reduction as terminal electron acceptor through the dissimilatory sulfate reduction (Eq. (2)) (Dou et al., 2020). The production of the sulfide in the microcosms was also inferred by the characteristic rotten egg smell in the microcosms (He et al., 2011). Interestingly, Salehi Alaei et al. (2023) observed the conversion of copper oxides (Cu₂O) to Cu₂S by a chemical substitution reaction between sulfide and the oxide (Eq. (3)). Additionally, Dou et al. (2020) proposed that the resulting metabolite HS⁻, from H₂S secreted by SRB, can diffuse to the surface and react with copper to form Cu₂S (Eq. (4)).



Chen et al. (2014) demonstrated that under anoxic conditions, SRB can form a Cu₂S film as the primary corrosion product. The production of extracellular polymeric substances (EPS) from the SRB biofilm, and subsequently the Cu₂S film, mitigates the toxicity of copper toward SRB.

In experiments with copper and different SRB strains, Kurmakova et al. (2019) found that these bacteria were accountable for Cu₂S corrosion products, with *Desulfovibrio* sp. M.4.1 showing the highest corrosive impact on the metal surface. The corrosion of high-purity copper in the presence of SRB in groundwater borehole or MX-80 clay has been demonstrated in other studies, where the presence of Cu₂S precipitates was detected (Johansson et al., 2017; Masurat et al., 2010). The addition of acetate, lactate, and sulfate to Spanish bentonite has been demonstrated to enhance bacterial activity, leading to the development of small corrosion compounds on copper discs within compacted bentonite blocks in the absence of water flow renewal after one year of anoxic incubation (Martinez-Moreno et al., 2023). The presence of an aqueous phase (EW) in this study accelerated this process, with corrosion compound formation observed in an early-stage of incubation (45 days).

4. Study overview and conclusions

The surrounded environment of future DGR is considered hostile to organisms' survival (e.g., high temperature due to heat generated by the decay process of the radionuclides, low water activity close to the canisters, high compaction of the bentonite, etc.). All these possible scenarios should be considered when assessing the release of radionuclides and their migration to the biosphere over periods of time spanning hundreds of thousands to millions of years. Here, ideal conditions for microorganism's survival and activity, bentonite slurry microcosms amended with electron donors/acceptor, were simulated. Although the DGR is designed to hinder the diffusion of pore water into the canisters, the flow of nutrients within the groundwater is not discarded. Consequently, examining laboratory-scale models is crucial in generating new insights on the biogeochemical processes under different scenarios.

This study describes the geochemical evolution of the bentonite slurry microcosms over a year-long anaerobic incubation at 28 °C, and in an early-stage (45 days) microbial-community characterization and its influence in the corrosion of copper material. A trend towards pH stabilization was observed, which could be linked to the biotic processes (generation of biogenic gases like H₂, CH₄, or CO₂) and the buffering properties of the bentonite. The consumption of lactate was the most pronounced, coupled with the formation of acetate and hydrogen sulfide in the microcosms. These findings were supported by the observation of fissures in the bentonite and the smell of rotten eggs after sampling. Moreover, the produced sulfide can react with the iron within the bentonite, causing their color shift to grayish-blackish hues. It is important to highlight that the ideal conditions consisted in amended bacterial consortium and electron donors/acceptor, significantly accelerated biogeochemical processes, whereas the tyndallization of the bentonite had a retarding effect.

The amended BPAS consortium was found to reduce the microbial diversity in the microcosms at the early stage (45 days), with *Pseudomonas* and *Stenotrophomonas* emerging as the predominant bacteria. Conversely, microcosms lacking BPAS consortium and amended with electron donors/acceptor or with heat-shocked bentonite exhibited higher microbial diversity and heterogeneity. However, the addition of electron donors/acceptor helped with the stimulation of certain bacterial groups such as SRB, playing an important role in the formation of corrosion products on the copper surface.

Under anaerobic conditions, SRB are capable of oxidizing electron donors (e.g., lactate) coupled to sulfate reduction through dissimilatory sulfate reduction pathway. The produced sulfide could mediate the conversion of copper oxides (possibly formed by trapped oxygen molecules on the bentonite or driven by the reduction of H₂O from the EW) to copper sulfide (Cu₂S) by a chemical substitution reaction between sulfides and oxides, or by the diffusion of and reaction of HS⁻ with copper.

Overall, microorganisms will play an important role in the geochemical evolution within the DGR and the stability of the different barriers could be compromised, emphasizing the impact of the SRB on the corrosion of the metal canisters, the gas generation, and the

interaction with components of the bentonite.

Funding

The present work was supported by the grant RTI 2018–101548-B-I00 “ERDF A way of making Europe” to MLM from the “Ministerio de Ciencia, Innovación y Universidades” (Spanish Government). The project leading to this application has received funding from the European Union’s Horizon 2020 research and innovation program under grant agreement No 847593 to MLM. ADM acknowledges funding from the UK Engineering and Physical Sciences Research Council (EPSRC) DTP scholarship (project reference: 2748843).

CRediT authorship contribution statement

Marcos F. Martínez-Moreno: Writing – review & editing, Writing – original draft, Visualization, Validation, Project administration, Methodology, Investigation, Formal analysis, Data curation, Conceptualization. **Cristina Povedano-Priego:** Writing – review & editing, Validation, Methodology, Conceptualization. **Mar Morales-Hidalgo:** Writing – review & editing, Validation, Conceptualization. **Adam D. Mumford:** Writing – review & editing, Validation, Investigation, Formal analysis, Data curation. **Elisabet Aranda:** Writing – review & editing, Resources, Formal analysis, Data curation. **Fadwa Jroundi:** Writing – review & editing, Validation, Conceptualization. **Jesus J. Ojeda:** Writing – review & editing, Validation, Supervision, Resources, Investigation, Formal analysis, Conceptualization. **Mohamed L. Merroun:** Writing – review & editing, Validation, Supervision, Resources, Project administration, Methodology, Funding acquisition, Conceptualization.

Declaration of competing interest

The authors declare that they have no known competing financial interests or personal relationships that could have appeared to influence the work reported in this paper.

Data availability

Data will be made available on request.

Acknowledgements

The authors acknowledge the assistance of Dr. F. Javier Huertas (IACT, Spain) for his guidance and help in collecting the bentonite from the El Cortijo de Archidona site (Almería). Rahul N. Doulatram Gargam and Maria del Carmen Contreras Morales (Institute of Water Research, University of Granada) for HPIC measurements. Moreover, Daniel García-Muñoz Bautista-Cerro and Alicia González Segura (Centro de Instrumentación Científica, University of Granada, Spain) for the sample preparation and microscopy assistance, respectively. Funding for open access charge: Universidad de Granada / CBUA

Appendix A. Supplementary data

Supplementary data to this article can be found online at <https://doi.org/10.1016/j.envpol.2024.124491>.

References

- Bagnoud, A., De Bruijn, I., Andersson, A.F., Diomidis, N., Leupin, O.X., Schwyn, B., Bernier-Latmani, R., 2016. A minimalistic microbial food web in an excavated deep subsurface clay rock. *FEMS Microbiol. Ecol.* 92 (1), fiv138 <https://doi.org/10.1093/femsec/fiv138>.
- Batandjieva, B., Delcheva, T., Duhovnik, B., 2009. Classification of Radioactive Waste: Safety Guide: IAEA General Safety Guide GSG-1. International Atomic Energy Agency, Vienna.
- Bengtsson, A., Pedersen, K., 2017. Microbial sulphide-producing activity in water saturated Wyoming MX-80, Asha and Calcigel bentonites at wet densities from 1500 to 2000 kg m⁻³. *Appl. Clay Sci.* 137, 203–212. <https://doi.org/10.1016/j.clay.2016.12.024>.
- Burzan, N., Murad Lima, R., Fruttschi, M., Janowczyk, A., Reddy, B., Rance, A., et al., 2022. Growth and persistence of an aerobic microbial Community in Wyoming Bentonite MX-80 despite anoxic in situ conditions. *Front. Microbiol.* 13, 858324 <https://doi.org/10.3389/fmicb.2022.858324>.
- Cheng, S., Li, N., Jiang, L., Li, Y., Xu, B., Zhou, W., 2019. Biodegradation of metal complex Naphthol Green B and formation of iron–sulfur nanoparticles by marine bacterium *Pseudalteromonas* sp CF10-13. *Bioresour. Technol.* 273, 49–55. <https://doi.org/10.1016/j.biortech.2018.10.082>.
- Chen, S., Wang, P., Zhang, D., 2014. Corrosion behavior of copper under biofilm of sulfate-reducing bacteria. *Corrosion Sci.* 87, 407–415. <https://doi.org/10.1016/j.corsci.2014.07.001>.
- Clarke, T.A., Rizkalla, E.N., 1976. X-ray photoelectron spectroscopy of some silicates. *Chem. Phys. Lett.* 37 (3), 523–526. [https://doi.org/10.1016/0009-2614\(76\)85029-4](https://doi.org/10.1016/0009-2614(76)85029-4).
- Cross, M.M., Manning, D.A., Bottrell, S.H., Worden, R.H., 2004. Thermochemical sulphate reduction (TSR): experimental determination of reaction kinetics and implications of the observed reaction rates for petroleum reservoirs. *Org. Geochem.* 35, 393–404. <https://doi.org/10.1016/j.orggeochem.2004.01.005>.
- Dou, W., Pu, Y., Han, X., Song, Y., Chen, S., Gu, T., 2020. Corrosion of Cu by a sulfate reducing bacterium in anaerobic vials with different headspace volumes. *Bioelectrochemistry* 133, 107478. <https://doi.org/10.1016/j.bioelechem.2020.107478>.
- Eschbach, M., Schreiber, K., Trunk, K., Buer, J., Jahn, D., Schobert, M., 2004. Long-term anaerobic survival of the opportunistic pathogen *Pseudomonas aeruginosa* via pyruvate fermentation. *J. Bacteriol.* 186 (14), 4596–4604. <https://doi.org/10.1128/jb.186.14.4596-4604.2004>.
- Essén, S.A., Johnsson, A., Bylund, D., Pedersen, K., Lundstrom, U.S., 2007. Siderophore production by *Pseudomonas stutzeri* under aerobic and anaerobic conditions. *Appl. Environ. Microbiol.* 73 (18), 5857–5864. <https://doi.org/10.1128/AEM.00072-07>.
- Fairley, N., 2019. CasaXPS, 2.3.22 ed. Casa Software Ltd.
- Fernández, A.M., 2004. Caracterización y modelización del agua intersticial de materiales arcillosos: Estudio de la bentonita de Cortijo de Archidona. Editorial Ciemat. ISBN84-7834-479-9 505.
- Freikowski, D., Winter, J., Gallert, C., 2010. Hydrogen formation by an arsenate-reducing *Pseudomonas putida*, isolated from arsenic-contaminated groundwater in West Bengal, India. *Appl. Microbiol. Biotechnol.* 88, 1363–1371. <https://doi.org/10.1007/s1201000988520>.
- García-Romero, E., María Manchado, E., Suárez, M., García-Rivas, J., 2019. Spanish bentonites: a review and new data on their geology, mineralogy, and crystal chemistry. *Fortschr. Mineral.* 9, 696. <https://doi.org/10.3390/min9110696>.
- Guo, G., Fall, M., 2021. Advances in modelling of hydro-mechanical processes in gas migration within saturated bentonite: a state-of-art review. *Eng. Geol.* 287, 106123 <https://doi.org/10.1016/j.enggeo.2021.106123>.
- Hall, D.S., Behazin, M., Binns, W.J., Keech, P.G., 2021. An evaluation of corrosion processes affecting copper-coated nuclear waste containers in a deep geological repository. *Prog. Mater. Sci.* 118, 100766 <https://doi.org/10.1016/j.pmatsci.2020.100766>.
- Hammer, O., 2001. PAST: paleontological statistics software package for education and data analysis. *Palaeontol. Electron.* <http://palaeo-electronica.org>.
- He, R., Xia, F.F., Wang, J., Pan, C.L., Fang, C.R., 2011. Characterization of adsorption removal of hydrogen sulfide by waste biocover soil, an alternative landfill cover. *J. Hazard Mater.* 186 (1), 773–778. <https://doi.org/10.1016/j.jhazmat.2010.11.062>.
- Hippe, H., Stackebrandt, E., 2015. *Desulfosporosinus*. *Bergey’s Manual of Systematics of Archaea and Bacteria*, pp. 1–10. <https://doi.org/10.1002/9781118960608.gbm00660>.
- Hong, H., Kim, S.J., Min, U.G., Lee, Y.J., Kim, S.G., Roh, S.W., et al., 2015. *Anaerobibacter carboniphilus* gen. nov., sp. nov., a strictly anaerobic iron-reducing bacterium isolated from coal-contaminated soil. *Int. J. Syst. Evol. Microbiol.* 65 (Pt 5), 1480–1485. <https://doi.org/10.1099/ijs.0.000124>.
- Huertas, F., Farina, P., Farias, J., García-Siñeriz, J.L., Villar, M.V., Fernández, A.M., Martín, P.L., Elorza, F.J., Gens, A., Sánchez, M., Lloret, A., Samper, J., Martínez, M.Á., 2021. Full-scale engineered barriers experiment. Updated Final Report 1994-2004. 2, 37-51.
- Huttunen-Saarivirta, E., Rajala, P., Carpen, L., 2016. Corrosion behaviour of copper under biotic and abiotic conditions in anoxic ground water: electrochemical study. *Electrochim. Acta* 203, 350–365. <https://doi.org/10.1016/j.electacta.2016.01.098>.
- Ishii, S., Ashida, N., Ohno, H., Segawa, T., Yabe, S., Otsuka, S., et al., 2017. *Noviherbaspirillum denitrificans* sp. nov., a denitrifying bacterium isolated from rice paddy soil and *Noviherbaspirillum autotrophicum* sp. nov., a denitrifying, facultatively autotrophic bacterium isolated from rice paddy soil and proposal to reclassify *Herbaspirillum massiliense* as *Noviherbaspirillum massiliense* comb. nov. *Int. J. Syst. Evol. Microbiol.* 67 (6), 1841–1848. <https://doi.org/10.1099/ijs.0.001875>.
- Johansson, A.J., Lilja, C., Sjögren, L., Gordon, A., Hallbeck, L., Johansson, L., 2017. Insights from post-test examination of three packages from the MiniCan test series of coppercast iron canisters for geological disposal of spent nuclear fuel: impact of the presence and density of bentonite clay. *Corrosion Eng. Sci. Technol.* 52, 54–60. <https://doi.org/10.1080/1478422X.2017.1296224>.
- Keech, P.G., Vo, P., Ramamurthy, S., Chen, J., Jacklin, R., Shoesmith, D.W., 2014. Design and development of copper coatings for long term storage of used nuclear fuel. *Corrosion Eng. Sci. Technol.* 49 (6), 425–430. <https://doi.org/10.1179/1743278214Y.0000000206>.

- Krylova, V., Andrulevičius, M., 2009. Optical, XPS and XRD studies of semiconducting copper sulfide layers on a polyamide film. *Int. J. Photoenergy*. <https://doi.org/10.1155/2009/304308>.
- Kurmakova, I., Kupchyk, O., Bondar, O., Demchenko, N., Vorobyova, V., 2019. Corrosion of copper in a medium of bacteria sulfate reduction proceeding. *J. Chem. Technol. Metall.* 54 (2), 416–422, 2019.
- Kutty, T.R.N., 1991. A controlled copper-coating method for the preparation of ZnS: Mn DC electroluminescent powder phosphors. *Mater. Res. Bull.* 26 (5), 399–406. [https://doi.org/10.1016/0025-5408\(91\)90054-P](https://doi.org/10.1016/0025-5408(91)90054-P).
- Liesack, W., Finster, K., 1994. Phylogenetic analysis of five strains of gram-negative, obligately anaerobic, sulfur-reducing bacteria and description of *Desulfuromusa* gen. nov., including *Desulfuromusa kysingii* sp. nov., *Desulfuromusa bakii* sp. nov., and *Desulfuromusa succinoxidans* sp. nov. *Int. J. Syst. Evol. Microbiol.* 44 (4), 753–758. <https://doi.org/10.1099/00207713-44-4-753>.
- Liu, D., Dong, H., Bishop, M.E., Zhang, J., Wang, H., Xie, S., Wang, S., Huang, L., Eberl, D.D., 2012. Microbial reduction of structural iron in interstratified illite-smectite minerals by a sulfate-reducing bacterium. *Geobiology* 10, 150–162. <https://doi.org/10.1111/j.1472-4669.2011.00307.x>.
- Martínez-Moreno, M.F., Povedano-Priego, C., Morales-Hidalgo, M., Mumford, A.D., Ojeda, J.J., Jroundi, F., Merroun, M.L., 2023. Impact of compacted bentonite microbial community on the clay mineralogy and copper canister corrosion: a multidisciplinary approach in view of a safe Deep Geological Repository of nuclear wastes. *J. Hazard Mater.* 131940 <https://doi.org/10.1016/j.jhazmat.2023.131940>.
- Martínez-Moreno, M.F., Povedano-Priego, C., Mumford, A.D., Morales-Hidalgo, M., Mijnenonckx, K., Jroundi, F., Merroun, M.L., 2024. Microbial responses to elevated temperature: Evaluating bentonite mineralogy and copper canister corrosion within the long-term stability of deep geological repositories of nuclear waste. *Science of the Total Environment* 915, 170149. <https://doi.org/10.1016/j.scitotenv.2024.170149>.
- Masurat, P., Eriksson, S., Pedersen, K., 2010. Microbial sulphide production in compacted Wyoming bentonite MX-80 under in situ conditions relevant to a repository for high-level radioactive waste. *Appl. Clay Sci.* 47, 58–64. <https://doi.org/10.1016/j.clay.2009.01.004>.
- Matschiavelli, N., Kluge, S., Podlech, C., Standhaft, D., Grathoff, G., Ikeda-Ohno, A., Cherkouk, A., 2019. The year-long development of microorganisms in uncompacted bavarian bentonite slurries at 30 and 60 °C. *Environ. Sci. Technol.* 2019 53, 10514–10524. <https://doi.org/10.1021/acs.est.9b02670>.
- Meleshyn, A., 2014. Microbial processes relevant for the long-term performance of high-level radioactive waste repositories in clays. *Geological Society, London, Special Publications* 400 (1), 179–194. <https://doi.org/10.1144/SP400.6>.
- Miettinen, H., Bomberg, M., Bes, R., Tiljander, M., Vikman, M., 2022. Transformation of inherent microorganisms in Wyoming-type bentonite and their effects on structural iron. *Appl. Clay Sci.* 221, 106465 <https://doi.org/10.1016/j.clay.2022.106465>.
- Oh, Y.S., Park, A.R., Lee, J.K., Lim, C.S., Yoo, J.S., Roh, D.H., 2011. *Pseudoalteromonas donghaensis* sp. nov., isolated from seawater. *Int. J. Syst. Evol. Microbiol.* 61 (2), 351–355. <https://doi.org/10.1099/ijs.0.022541-0>.
- Ojovan, M.I., Steinmetz, H.J., 2022. Approaches to disposal of nuclear waste. *Energies* 15, 7804. <https://doi.org/10.3390/en15207804>.
- Park, S.Y., Zhang, Y., O'Loughlin, E.J., Jo, H.Y., Kwon, J.S., Kwon, M.J., 2024. Temperature-dependent microbial reactions by indigenous microbes in bentonite under Fe (III)- and sulfate-reducing conditions. *J. Hazard Mater.* 465, 133318 <https://doi.org/10.1016/j.jhazmat.2023.133318>.
- Payer, J.H., Finsterle, S., Apps, J.A., Muller, R.A., 2019. Corrosion performance of engineered barrier system in deep horizontal drillholes. *Energies* 12, 1491. <https://doi.org/10.3390/en12081491>.
- Pentáková, L., Su, K., Penták, M., Stucki, J.W., 2013. A review of microbial redox interactions with structural Fe in clay minerals. *Clay Miner.* 48, 543–560. <https://doi.org/10.1180/claymin.2013.048.3.10>.
- Povedano-Priego, C., Jroundi, F., Solari, P.L., Guerra-Tschuschke, I., del Mar Abad-Ortega, M., Link, A., et al., 2023. Unlocking the bentonite microbial diversity and its implications in selenium bioreduction and biotransformation: advances in deep geological repositories. *J. Hazard Mater.* 445, 130557 <https://doi.org/10.1016/j.jhazmat.2022.130557>.
- Povedano-Priego, C., Jroundi, F., Lopez-Fernandez, M., Shrestha, R., Spanek, R., Martín-Sánchez, I., Villar, M.V., Sevcú, A., Dopson, M., Merroun, M.L., 2021. Deciphering indigenous bacteria in compacted bentonite through a novel and efficient DNA extraction method: insights into biogeochemical processes within the Deep Geological Disposal of nuclear waste concept. *J. Hazard Mater.* 408, 124600 <https://doi.org/10.1016/j.jhazmat.2020.124600>.
- Povedano-Priego, C., Jroundi, F., Lopez-Fernandez, M., Sánchez-Castro, I., Martín-Sánchez, I., Huertas, F.J., Merroun, M.L., 2019. Shifts in bentonite bacterial community and mineralogy in response to uranium and glycerol-2-phosphate exposure. *Sci. Total Environ.* 692, 219–232. <https://doi.org/10.1016/j.scitotenv.2019.07.228>.
- Qin, Q.L., Li, Y., Zhang, Y.J., Zhou, Z.M., Zhang, W.X., Chen, X.L., et al., 2011. Comparative genomics reveals a deep-sea sediment-adapted life style of *Pseudoalteromonas* sp. SM9913. *ISME J.* 5, 274–284. <https://doi.org/10.1038/ismej.2010.103>.
- R Core Team, 2022. R: A Language and Environment for Statistical Computing. R Foundation for Statistical Computing, Vienna, Austria. URL: <https://www.R-project.org/>.
- Robertson, C.E., Harris, J.K., Wagner, B.D., Granger, D., Browne, K., Tatem, B., Feazel, L. M., Park, K., Pace, N.R., Frank, D.N., 2013. Explicit: graphical user interface software for metadata-driven management, analysis and visualization of microbiome data. *Bioinformatics* 29, 3100–3101. <https://doi.org/10.1093/bioinformatics/btt526>.
- Rozalén, M., Brady, P.V., Huertas, F.J., 2009. Surface chemistry of K-montmorillonite: ionic strength, temperature dependence and dissolution kinetics. *J. Colloid Interface Sci.* 333 (2), 474–484. <https://doi.org/10.1016/j.jcis.2009.01.059>.
- Ruiz-Fresneda, M.A., Martínez-Moreno, M.F., Povedano-Priego, C., Morales-Hidalgo, M., Jroundi, F., Merroun, M.L., 2023. Impact of microbial processes on the safety of deep geological repositories for radioactive waste. *Front. Microbiol.* 14, 1134078. <https://doi.org/10.3389/fmicb.2023.1134078>.
- Ruiz-Fresneda, M.A., Gomez-Bolivar, J., Delgado-Martin, J., Abad-Ortega, M.D.M., Guerra-Tschuschke, I., Merroun, M.L., 2019. The bioreduction of selenium under anaerobic and alkaline conditions analogous to those expected for a deep geological repository system. *Molecules* 24 (21), 3868. <https://doi.org/10.3390/molecules24213868>.
- Salehi Alaei, E., Guo, M., Chen, J., Behazin, M., Bergendal, E., Lilja, C., et al., 2023. The transition from used fuel container corrosion under oxidic conditions to corrosion in an anoxic environment. *Mater. Corros.* 74 (11–12), 1690–1706. <https://doi.org/10.1002/maco.202313757>.
- Sanchez-Castro, I., Ruiz-Fresneda, M.A., Bakkali, M., Kämpfer, P., Glaeser, S.P., Busse, H. J., et al., 2017. *Stenotrophomonas bentonitica* sp. nov., isolated from bentonite formations. *Int. J. Syst. Evol. Microbiol.* 67 (8), 2779. [10.1099%2Fijsem.0.002016](https://doi.org/10.1099%2Fijsem.0.002016).
- Sanford, R.A., Cole, J.R., Tiedje, J.M., 2002. Characterization and description of *Anaeromyxobacter dehalogenans* gen. nov. sp. nov., an aryl-halo-respiring facultative anaerobic myxobacterium. *Appl. Environ. Microbiol.* 68 (2), 893–900. <https://doi.org/10.1128/AEM.68.2.893-900.2002>.
- Schutz, M.K., Schlegel, M.L., Libert, M., Bildstein, O., 2015. Impact of iron-reducing bacteria on the corrosion rate of carbon steel under simulated geological disposal conditions. *Environ. Sci. Technol.* 49 (12), 7483–7490. <https://doi.org/10.1021/acs.est.5b00693>.
- Shelobolina, E.S., VanPraagh, C.G., Lovley, D.R., 2003. Use of ferric and ferrous iron containing minerals for respiration by *Desulfitobacterium frapperi*. *Geomicrobiol. J.* 20, 143–156. <https://doi.org/10.1080/01490450303884>.
- Shiratori-Takano, H., Akita, K., Yamada, K., Itoh, T., Sugihara, T., Beppu, T., Ueda, K., 2014. Description of *Symbiobacterium ostreiconchae* sp. nov., *Symbiobacterium turbinis* sp. nov. and *Symbiobacterium terraclatae* sp. nov., isolated from shellfish, emended description of the genus *Symbiobacterium* and proposal of *Symbiobacteriaceae* fam. nov. *Int. J. Syst. Evol. Microbiol.* 64 (Pt 10), 3375–3383. <https://doi.org/10.1099/ijs.0.063750-0>.
- Shrestha, R., Cerna, K., Spanek, R., Bartak, D., Cernousek, T., Sevcu, A., 2022. The effect of low-pH concrete on microbial community development in bentonite suspensions as a model for microbial activity prediction in future nuclear waste repository. *Sci. Total Environ.* 808, 151861 <https://doi.org/10.1016/j.scitotenv.2021.151861>.
- Spring, S., Sorokin, D.Y., Verburg, S., Rohde, M., Woyke, T., Kyrpides, N.C., 2019. Sulfate-reducing bacteria that produce exopolymers thrive in the calcifying zone of a hypersaline cyanobacterial mat. *Front. Microbiol.* 10, 862. <https://doi.org/10.3389/fmicb.2019.00862>.
- Spring, S., Rosenzweig, F., 2006. The genera *Desulfitobacterium* and *Desulfosporosinus*: taxonomy. *The prokaryotes* 4, 771–786. https://doi.org/10.1007/0-387-30744-3_24.
- Stackebrandt, E., Sproer, C., Rainey, F.A., Burghardt, J., Pücker, O., Hippe, H., 1997. Phylogenetic analysis of the genus *Desulfotomaculum*: evidence for the misclassification of *Desulfotomaculum guttoideum* and description of *Desulfotomaculum orientis* as *Desulfosporosinus orientis* gen. nov., comb. nov. *Int. J. Syst. Evol. Microbiol.* 47 (4), 1134–1139. <https://doi.org/10.1099/00207713-47-4-1134>.
- Villar, M.V., Fernández-Soler, J.M., Delgado Huertas, A., Reyes, E., Linares, J., Jiménez de Cisneros, C., Linares, J., Reyes, E., Delgado, A., Fernández-Soler, J.M., Astudillo, J., 2006. The study of Spanish clays for their use as sealing materials in nuclear waste repositories: 20 years of progress. *J. Iber. Geol.* 32, 15–36.
- Wagner, C.D., Riggs, W.M., Davis, L.E., Moulder, J.F., Muilenberg, G.E., 1979. *Handbook of X-Ray Photoelectron Spectroscopy: a Reference Book of Standard Data for Use in X-Ray Photoelectron Spectroscopy*. Perkin-Elmer Corporation, Eden Prairie, MN.
- WNA. World Nuclear Association, 2021. Storage and disposal of radioactive waste. <https://www.world-nuclear.org/>.
- Yu, X.R., Liu, F., Wang, Z.Y., Chen, Y., 1990. Auger parameters for sulfur-containing compounds using a mixed aluminum-silver excitation source. *J. Electron. Spectrosc. Relat. Phenom.* 50 (2), 159–166. [https://doi.org/10.1016/0368-2048\(90\)87059-W](https://doi.org/10.1016/0368-2048(90)87059-W).